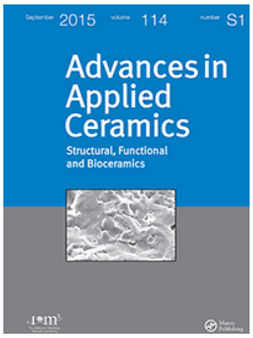

Advances in Applied Ceramics
Structural, Functional and Bioceramics

ISSN: 1743-6753 (Print) 1743-6761 (Online) Journal homepage: http://www.tandfonline.com/loi/yaac20

Characterisation of Bioglass based foams developed via replication of natural marine sponges

E. Boccardi, A. Philippart, J. A. Juhasz-Bortuzzo, G. Novajra, C. Vitale-Brovarone & A. R. Boccaccini

To cite this article: E. Boccardi, A. Philippart, J. A. Juhasz-Bortuzzo, G. Novajra, C. Vitale-Brovarone & A. R. Boccaccini (2015) Characterisation of Bioglass based foams developed via replication of natural marine sponges, Advances in Applied Ceramics, 114:sup1, S56-S62, DOI: 10.1179/1743676115Y.0000000036

To link to this article: http://dx.doi.org/10.1179/1743676115Y.0000000036

Published online: 02 Jul 2015.

RESEARCH PAPER

Characterisation of Bioglass based foams developed via replication of natural marine sponges

E. Boccardi[1], A. Philippart[1], J. A. Juhasz-Bortuzzo[1], G. Novajra[2], C. Vitale-Brovarone[2] and A. R. Boccaccini*[1]

A comparative characterisation of Bioglass based scaffolds for bone tissue engineering applications developed via a replication technique of natural marine sponges as sacrificial template is presented, focusing on their architecture and mechanical properties. The use of these sponges presents several advantages, including the possibility of attaining higher mechanical properties than those scaffolds made by foam replica method (up to 4 MPa) due to a decrease in porosity (68–76%) without affecting the pore interconnectivity (higher than 99%). The obtained pore structure possesses not only pores with a diameter in the range 150–500 μm, necessary to induce bone ingrowth, but also pores in the range of 0–200 μm, which are requested for complete integration of the scaffold and for neovascularisation. In this way, it is possible to combine the main properties that a three-dimensional scaffold should have for bone regeneration: interconnected and high porosity, adequate mechanical properties and bioactivity.

Keywords: Natural marine sponges, Bioglass, Replication technique

This paper is part of a special issue on glass and ceramic composites for high technology applications (GlaCERCo)

Introduction

One important tissue engineering branch involves the use of porous three-dimensional (3D) engineered scaffolds as an alternative to autografts and allografts to induce bone regeneration. The present 'gold standard' is to harvest 'donor' bone from a non-load bearing site and transplant it into the defect site of the same patient.[1] Using artificial porous 3D scaffolds, the aim is to reproduce the complex morphology of bone tissue using bioactive materials, which are able to integrate with the biological environment and promote the regeneration of natural tissue. The use of artificial scaffolds avoids the limitations of autografts, such as additional operating time, healing of both donor and implant sites, as well as pain and increased risk of infection at the donor site.[1–3] The challenge is the design of materials able to match not only the biological but also the mechanical properties of real bone tissue matrix and to support neovascularisation.[4,5] Bioglass 45S5, discovered by L. Hench in 1969, is one of the most important biomaterials for bone defect repair: it is a degradable silicate glass with a high content of calcium and is able to form a bond with both soft and hard tissues.[6,7] Indeed, when Bioglass is put in contact with biological fluids, a layer of carbonated hydroxyapatite similar to the mineral phase of bone is deposited on the surface and there is a release of silicon and calcium ions, which can stimulate the expression of several genes of osteoblastic cells and cause angiogenesis both *in vitro* and *in vivo*.[6,8–15]

Bioglass has been used in clinic for dental and orthopaedic applications in bulk form and as particulates in non-load bearing sites for bone grafting and for the prevention of dental hypersensitivity.[3,4,7] Porous 3D Bioglass based scaffolds are not yet available for clinical applications, although numerous techniques have been reported for the production of porous ceramics. Following the first study on fabrication of Bioglass based scaffolds by the foam replica method published in 2006,[16] other techniques have been proposed to make such scaffolds including foam replication,[16–18] sol–gel casting,[19,20] freeze drying,[21] 3D printing[22] and powder metallurgy.[23,24] One difficulty is the fabrication of a scaffold that has the same high porosity and sufficient mechanical strength and stability as natural bone. One approach could be the manufacture of Bioglass based scaffolds with enhanced mechanical properties by reducing the total porosity but without detrimentally affecting the pore interconnectivity. In recent years, 3D Bioglass based foams have been produced using a powder technology process developed by the National Research Council Canada—Industrial Material Institute.[23,24] Aguilar-Reyes *et al.* showed that foams with interconnected porosity (64–79% porosity) and with open pores in the 100–800 μm range can be produced with this process. The foams produced showed good mechanical strength (1.7–5.5 MPa) comparable with the compression strength of cancellous bone (2–12 MPa).[23,24] The achieved values[23,24] are notably higher than those obtained by the polyurethane (PU) sacrificial template method,[16]

[1]Institute of Biomaterials, Friedrich-Alexander Universität Erlangen-Nürnberg, Erlangen-Nürnberg, Germany
[2]Institute of Material Physics and Engineering, Department of Applied Sciences and Technologies, Politecnico di Torino, Torino, Italy

*Corresponding author, email aldo.boccaccini@ww.uni-erlangen.de

Received 09 February 2015; accepted 27 May 2015
DOI 10.1179/1743676115Y.0000000036

which exhibits higher porosity. The replication of a PU sacrificial template produces a porous structure that closely resembles that of cancellous bone, highly porous and interconnected structure with up to 95% porosity. However, the low mechanical properties, of only up to 2 MPa, limit its suitability for clinical applications. In an early effort, Cunningham *et al.* used marine natural sponges as sacrificial templates for the production of hydroxyapatite based scaffolds in place of PU foam.[25] They were able to obtain scaffolds with high open porosity and improved mechanical properties. Additionally, these scaffolds had pores in the range of 0–200 μm, which have been reported as being necessary for the complete integration of a bone substitute in natural tissue.[26–29] However, to the authors' knowledge, no further developments have been reported on this material. In the present work, the production of Bioglass based scaffolds using marine natural sponges, *Spongia agaricina* (SA) and *Spongia lamella* (SL), as template materials was investigated. These sponges, thanks to the millenarian evolution for water filtration, could be potential precursors in the production of bone tissue engineering scaffolds due to their efficient interconnected porous architecture.[30] The final aim of the present work was thus to obtain Bioglass based scaffolds with reduced total porosity and, consequently, increased mechanical properties, without the loss of interconnectivity of the pores essential for successful bone ingrowth.[25,27]

Experimental

Scaffold preparation

The starting material was melt derived 45S5 Bioglass powder (particle size 5 μm). The templates for the scaffold production were PU packaging foams (45 ppi) purchased from Eurofoam Deutschland GmbH Schaumstoffe and marine sponges SA and SL harvested respectively from the Indo-Pacific Ocean (Pure Sponges, UK) and Mediterranean Sea (Hygan Products Limited, UK) belonging to the 'Elephant Ear' family. Harvesting of all natural sponges has been performed in an environmentally friendly manner, as specified by the supplier companies. 45S5 Bioglass scaffolds were produced by the replica technique, according to the method described by Chen *et al.*[16] Briefly, the slurry for the scaffold fabrication was prepared by dissolving polyvinyl alcohol (PVA) in deionised water at 80°C for 1 h, the ratio being 0.01 mol L^{-1}. The 45S5 Bioglass was then added to 25 mL PVA–water solution with concentrations of up to 40 wt-%. Each procedure was carried out under vigorous stirring using a magnetic stirrer for 1 h. The sacrificial templates, cut into cylinders, were immersed into the slurry for 10 min. The foams were retrieved from the suspension, and the extra slurry was completely squeezed from the foam. The samples were then dried at room temperature for at least 12 h. This dip coating procedure was repeated two or three times to increase the coating thickness and, consequently, the mechanical properties of the scaffolds. After the second and third coating, the superfluous slurry was completely removed using compressed air. The PU foams and SL were immersed in the Bioglass powder slurry three times, while SA only required two coating cycles. The heat treatment required for the burn-out of the sacrificial template and sintering of the bioactive glass was carried out as reported in Fig. 1. The burn-out and sintering conditions were the same for all sacrificial templates, namely, 400°C/1 h and 1050°C/1 h respectively. The heating and the cooling down rates used were 2 and 5°C min^{-1} respectively.[16]

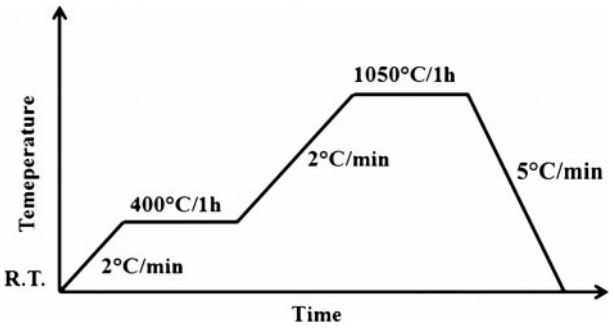

1 Thermal treatment: heat treatment programme designed for burning out templates and sintering 45S5 Bioglass green bodies

Characterisation

The density of the foams, ρ_{foams}, was measured using the mass and dimensions of the sintered cylinders. The porosity, p, was calculated using the formula:

$$p = \left(1 - \frac{\rho\,\text{foam}}{\rho\,\text{solid}}\right) * 100 \quad (1)$$

where $\rho_{solid} = 2.7$ g cm^{-3} (the theoretical density of 45S5 Bioglass not considering change of density due to crystallisation[31]).

The microstructure of the resulting scaffolds was investigated by means of a scanning electron microscopy (SEM) (Auriga 0750 Zeiss). The structure of the foams was observed using a micro-computed tomography (micro-CT) system (Skyscan 1147 Micro-CT). The pore interconnectivity was evaluated using CTan image analysis software. The pore size distribution was conducted on 2D sections extracted from micro-CT reconstructions using ImageJ analysis software.

The crystalline phases induced by the thermal treatment were identified by X-ray diffraction (XRD) measurements, carried out using a Philips Xpert diffractometer with a Cu K_α radiation source. The acquisition was performed in the range 10–70° two-theta with a 0.02° step size and dwell time/step time of 2 s. The diffraction lines were identified using X'Pert HigScore software.

The compression strength of the foams was measured using a Zwick Z050 mechanical tester at a crosshead speed of 1 mm min^{-1}, with a load cell of 50 N and 50 kN. Ten cylindrical samples, with dimensions of 7 mm in height and 5 mm in diameter, were tested. The load was applied until densification of the porous samples began to occur.

Results

Template and scaffold architecture

Images of all three templates are shown in Fig. 2, namely, PU packaging foam and two natural marine sponges (SA and SL). The mean PU foam pore size (Fig. 2*b*) was 770 ± 60 μm, and the thickness of the pore walls was 110 ± 15 μm. The SA and SL were characterised by a vase or fan shaped (Fig. 2*a*) growth and a surface composed by fine fibres. It was possible to recognise two different structures as reported by Pronzato and Manconi[30]: an inhalant (Fig. 2*c* and *d*) and an exhalant (Fig. 2*e* and *f*) surface, referred to the directionality of water flow in the sponges in their natural

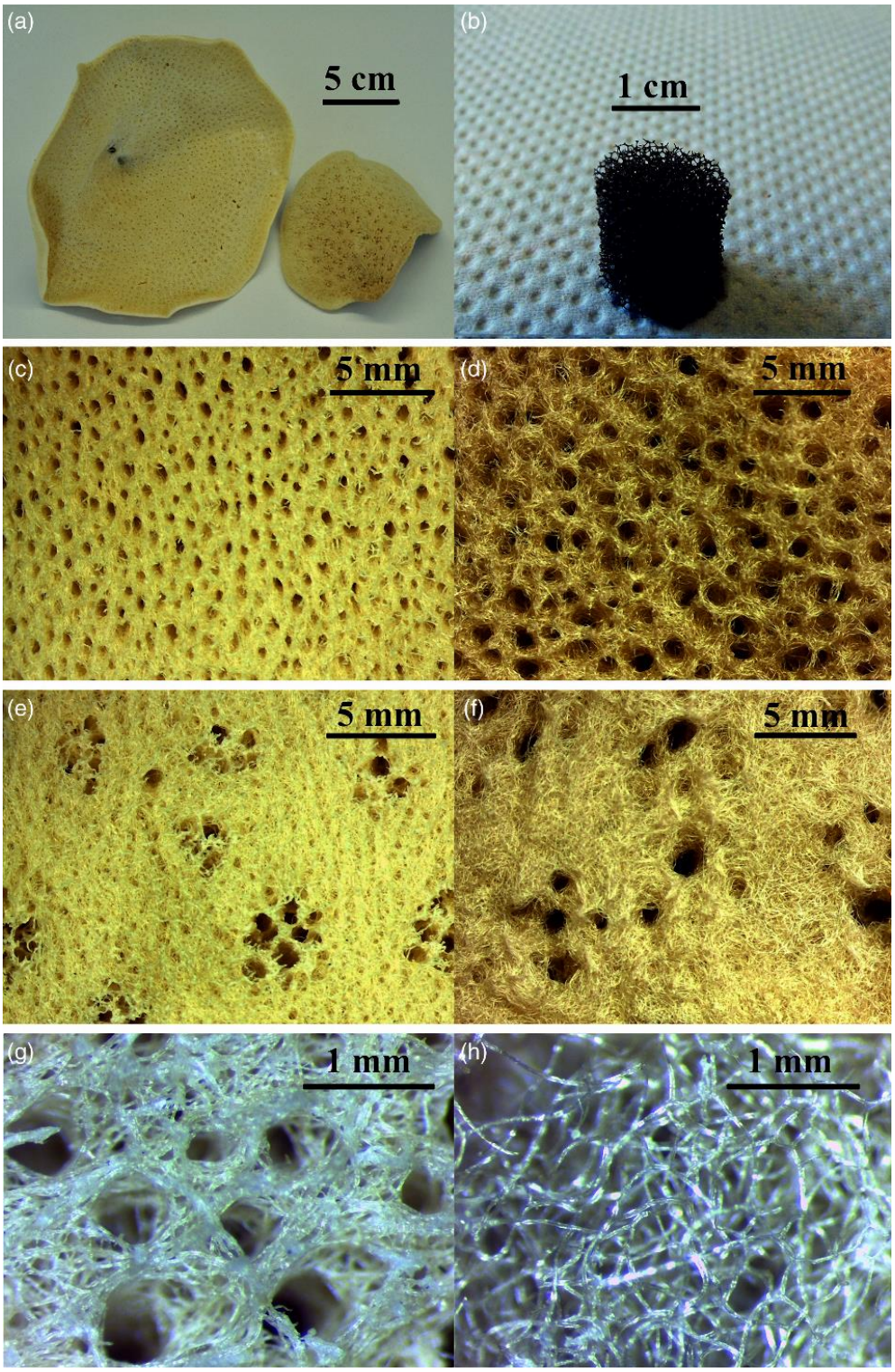

2 Natural marine sponge structure: digital camera images of Indo-Pacific (*a1*) and Mediterranean sponges (*a2*) and PU (*b*) templates; inhalant surfaces of Indo-Pacific (SA) (*c*) and Mediterranean (SL) (*d*) sponges; exhalant Indo-Pacific (SA) (*e*) and Mediterranean (SL) (*f*) sponges; fibrous network of Indo-Pacific (SA) (*g*) and Mediterranean Sea (SL) (*h*) sponges

habitat. The SL was composed of almost only primary fibres with a diameter of 35 ± 3 μm, while the SA was formed of a network of primary fibres (17 ± 3 μm) and an irregular network of secondary thicker fibres (63 ± 5 μm). The other main differences between these two marine sponges were (i) the wall pore thickness (540 ± 80 μm in SL and 420 ± 40 μm in SA) and (ii) the larger and more irregular pore structure of the SL sponges. The fibres formed a mesh of macropores in the inhalant surface (1.0 ± 0.1 mm in the SL and 590 ± 50 μm in the SA) and an almost regular cluster of five to seven pores on the exhalant surface (1.7 ± 0.2 mm in the SL and 920–90 μm in the SA). These results are summarised in Table 1. The obtained PU scaffolds (BG-PU) were characterised by a porosity of $93.00 \pm 0.25\%$, while the SL and SA replica foams (BG-SL and BG-SA respectively) had a porosity of $76 \pm 2\%$ and $68.0 \pm 0.2\%$, as determined by measurements of their mass and dimensions and applying equation (1). However, it is possible to observe from the

Table 1 Summary of natural marine sponge architecture properties: architectural properties of natural marine sponges are summarised, focusing on pore dimension and structural thickness

	Mediterranean Sea SL	Indian-Pacific Ocean SA
Pore dimension inhalant surface	1.0±0.1 mm	590±50 μm
Pore dimension exhalant surface	1.7±0.2 mm	920±90 μm
Pore wall thickness	540±80 μm	400±40 μm

SEM images reported in Fig. 3 that almost all the space between the fibrous structures of the marine sponges was filled with the Bioglass particles and the macropore patterns were perfectly replicated. In fact, it was still possible to distinguish the inhalant and exhalant surfaces of both types of sponge. Some small sized pores connecting the larger pores were also witnessed, forming an overall, highly interconnected porous structure.

Micro-CT analysis

Micro-CT analysis was employed to assess the interconnectivity of the porous network. It was also possible to calculate the strut thickness and the pore dimensions of the obtained 45S5 Bioglass based scaffolds. It was possible to observe from the pore size distribution analysis (Fig. 4) that when using PU as the sacrificial template, the resulting Bioglass based foams were characterised by a wide range of pore size from 100 to 900 μm, an average pore size 670±70 μm and a high level of interconnectivity (99.95%). The natural marine sponge foam replicas were characterised by a lower total porosity but, at the same time, by a very high pore interconnectivity (>99.5%). They contained pores in the range 0–600 μm and 0–900 μm and an average pore size

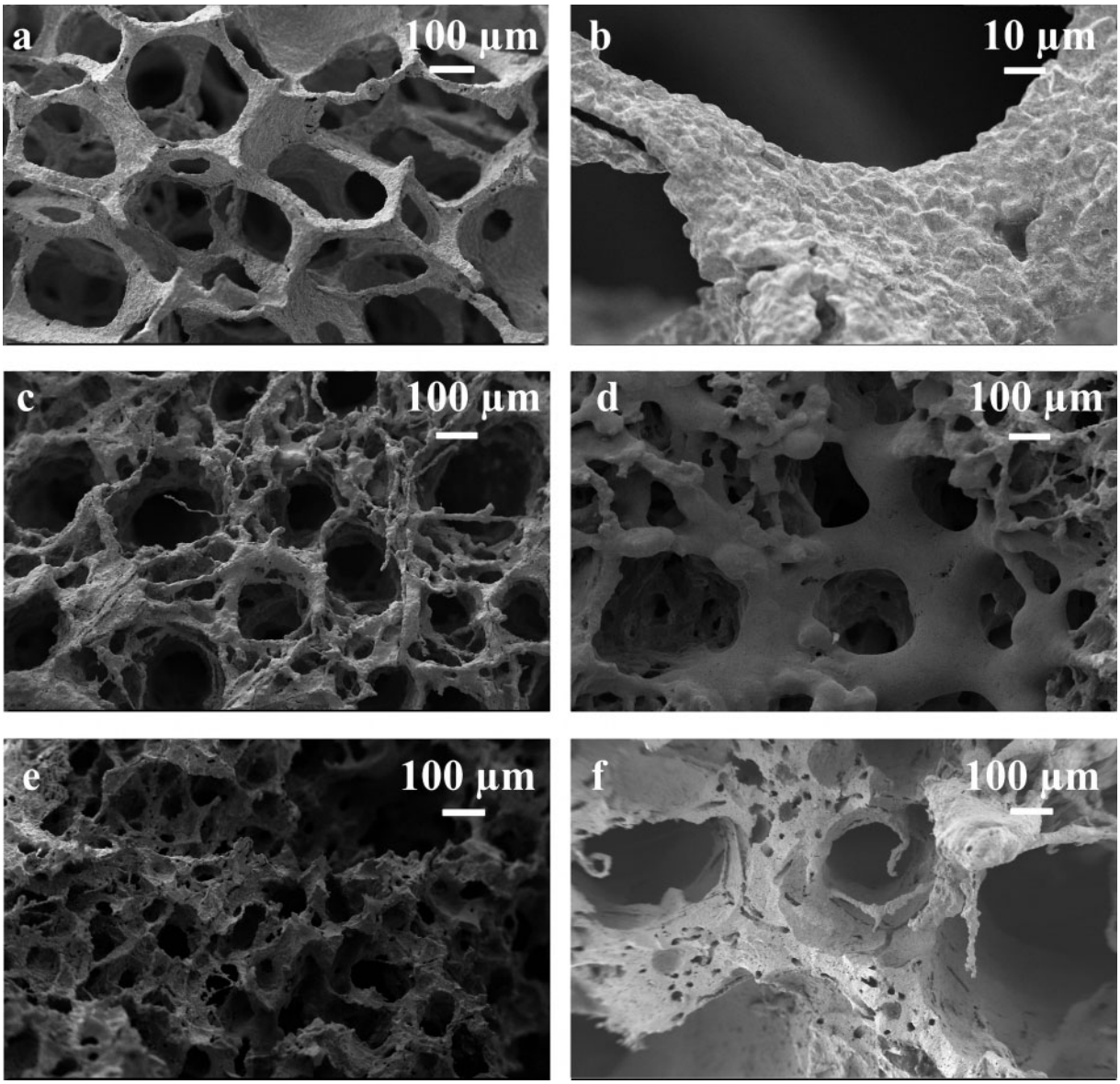

3 Bioglass based scaffolds: *a*, *b* PU replica foam (BG-PU) at different magnification; *c* inhalant surfaces and *d* exhalant surface of SA replica foam (BG-SA); *e*, *f* inhalant surfaces and exhalant surface of SL replica foam (BG-SL)

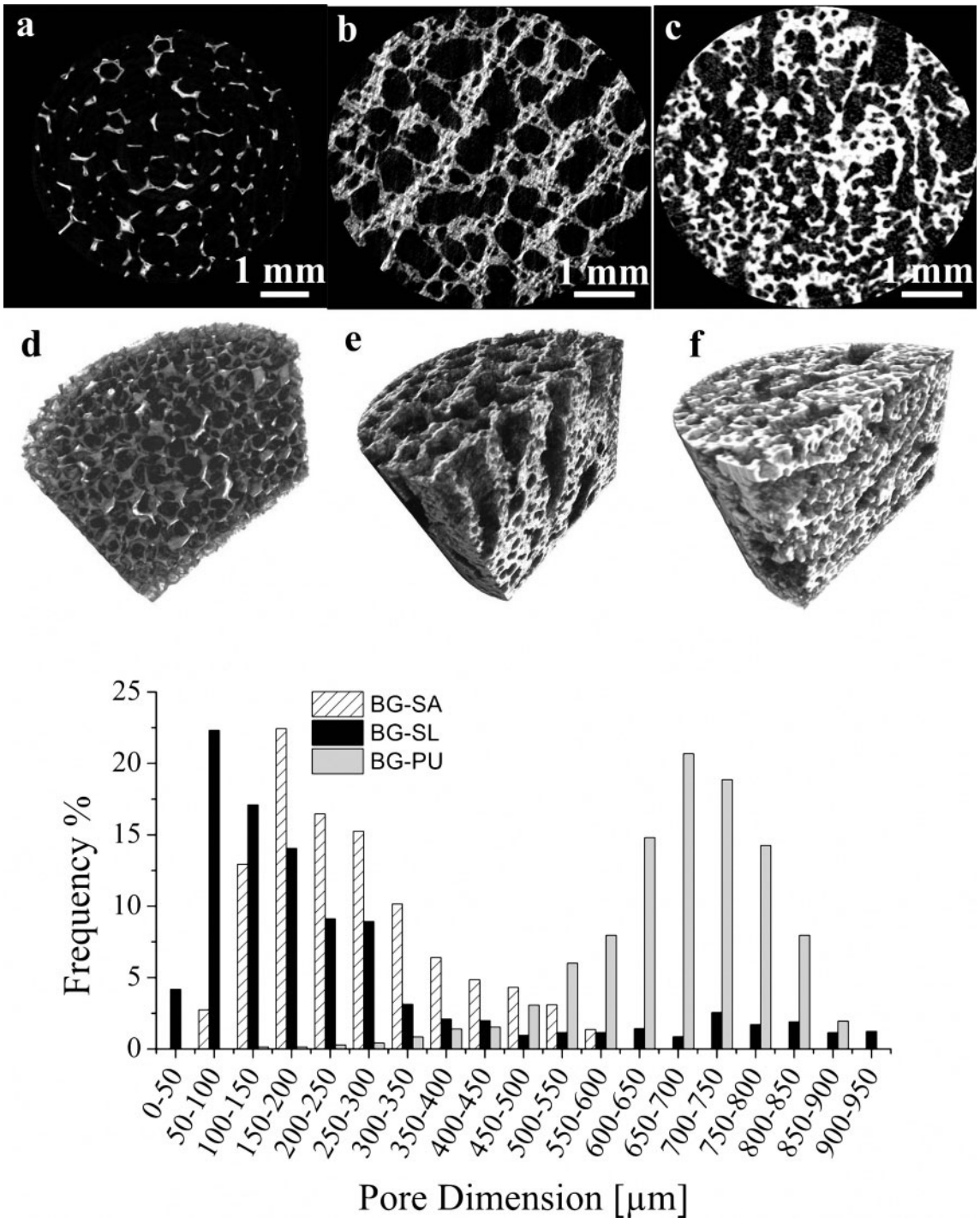

4 Micro-CT reconstructions: 2D section and 3D reconstruction of *a*, *d* BG-PU, *b*, *e* BG-SL and *f*, *g* BG-SA obtained by micro-CT analysis

of 215 ± 20 μm and 265 ± 120 μm for the BG-SA and BG-SL respectively. These foams also possessed significant microporosity, which was almost completely absent in the PU foam replicas, as summarised in Table 2. A 3D reconstruction of the micro-CT analysis in Fig. 4 provided images of their internal architecture, showing the highly interconnected porous network.

XRD analysis

The XRD analysis assessed the crystalline phase formation induced by the thermal treatment process. It was possible

Table 2 Bioglass based scaffold architectural properties: architectural properties of Bioglass based scaffolds prepared with PU and natural marine sponges as templates

	BG-PU	BG-SL	BG-SA
Pore interconnectivity/%	99.95	99.66	99.96
Average pore dimension/μm	670 ± 70	265 ± 20	215 ± 2.7
% Pores ⩽200 μm	2.7	38	56
% Pores within 150–500 μm	25	93	40
% Pores ⩾500 μm	80	5	16

to observe that the starting 45S5 Bioglass was completely amorphous, but after the sintering process, two crystalline phases formed. The main crystalline phase was combeite ($Na_2Ca_2Si_3O_9$) and the secondary phase, rhenanite ($CaNaPO_4$), as reported in Fig. 5. The same amorphous crystalline transformation was observed for all samples. The formation of combeite and rhenanite in sintered Bioglass structures has been discussed in literature.[32–34]

Mechanical testing

The maximum compressive strengths were recorded as being 1.8 ± 0.3 MPa for the BG-SL, 4.0 ± 0.4 MPa for BG-SA and < 0.05 MPa for the Bioglass scaffolds prepared using PU foam as template. Typical stress–deformation curves are shown in Fig. 6 for BG-SA and BG-SL. For BG-PU, the measurements were below the detection limit of the equipment.

Discussion

45S5 Bioglass, the original formulation of bioactive glasses identified by L. Hench in 1969,[6,7,35] is the most used bioactive glass in clinical applications as powders or bulk material.[7] So far, Bioglass based porous scaffolds have not been considered for load bearing applications due to their low mechanical properties.[7,35] In fact, it is still a challenge to obtain a Bioglass scaffold presenting at the same time good mechanical properties and high porosity.[35] In the present work, the possibility to increase the mechanical behaviour of Bioglass based scaffolds by reducing the total porosity was considered with natural marine sponges, SA and SL, chosen as sacrificial templates for the production of the scaffolds.[25,35] These sponges were characterised by a high interconnected porous structure made by fine fibres.[30] The architectural properties were well reproduced for SA; however, high variability in pore dimension and strut thickness was observed for SL. As a result of the high porosity of these natural marine sponges, the resulting Bioglass scaffolds were characterised by a very high interconnectivity of pores ($>99\%$). However, the total porosity was $\sim$18–20% lower than that of the samples obtained with the PU foam as sacrificial template. In addition, there was a significant amount of pores in the range of 0–200 μm, which were impossible to obtain using the PU template. Pores in this size range play an important role in the complete colonisation of the scaffolds by cells, enhancing the flow of biological fluids also in the inner core of the porous structure and the complete integration with the surrounding tissue.[26,27] Moreover, pores in the range of 200–500 μm were present, which are necessary for bone integration and neovascularisation.[26,27] As a main consequence of the reduction of the total porosity, there was an improvement of the mechanical properties up to 4 MPa for BG-SA and up to 1.8 MPa for SL. In the case of BG-PU, the resulting maximum compressive strength was lower than the average values found in literature ($\sim$0.4 MPa).[35] This was probably due to the compressed air used for the removal of the slurry excess after the second and third coating during scaffold preparation. Following this technique, it was easier to maintain an open porosity, but the amount of slurry removed was higher. The XRD results confirmed that the thermal treatment caused a modification of the Bioglass structure, inducing the formation of two crystalline phases: combeite ($Na_2Ca_2Si_3O_9$) as the main phase, as widely reported in literature,[16] and rhenanite ($CaNaPO_4$) as the secondary crystalline phase.[32–34] It was demonstrated that rhenanite can act as a heterogeneous nucleus for carbonated hydroxyapatite crystallisation in contact with simulated body fluid, and thus, it should improve the bioactivity of the material.[14,32,34,36]

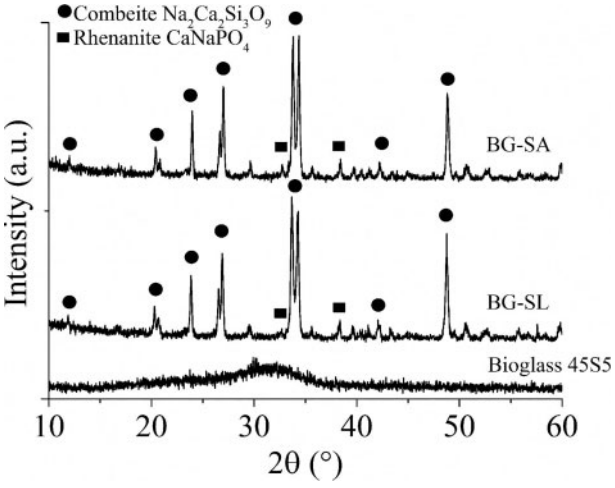

5 XRD of Bioglass scaffolds: XRD spectra of Bioglass 45S5, SL replica foam and SA foam replica

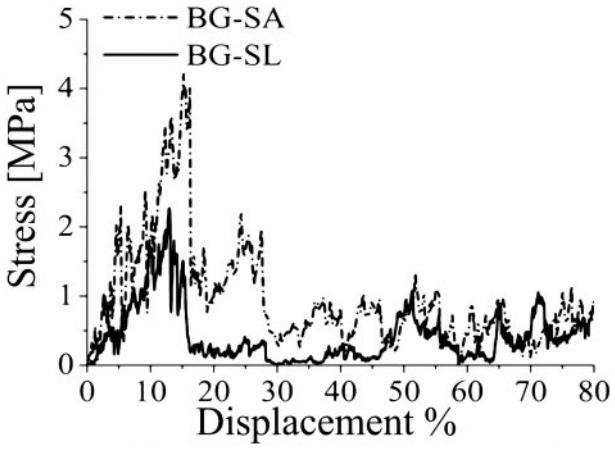

6 Mechanical properties: stress–displacement curves of Bioglass foams manufactured with different sacrificial templates

The achievement of improved mechanical behaviour, combined with the high pore interconnectivity and wide pore size distribution, confirmed the possibilities of using natural marine sponges from the Elephant Ear family as porous precursors for production of bone tissue scaffolds. The present results thus warrant further investigations on these scaffolds, in particular to characterise the scaffolds bioactivity, mechanical stability *in vitro* and *in vivo*, and oxygen diffusivity.

Conclusions

The use of natural marine sponges as sacrificial templates for porous Bioglass based scaffold preparation has been demonstrated as promising alternative to PU foams. The obtained scaffolds are characterised not only by the high interconnectivity of their porous structure but also by sound mechanical properties. In this way, it is possible to

combine the main properties (structural, mechanical and biological) that a 3D scaffold should have for bone regeneration.

Acknowledgement

This research was carried out in the framework of the EU ITN FP-7 project 'GlaCERCo'. The authors would like to acknowledge its financial support.

References

1. M. Stevenson: 'Biomaterials for bone tissue engineering', *Mater. Today*, 2008, **11**, (5), 18–25.
2. M. Vallet-Regì: 'Ordered mesoporous materials in the context of drug delivery systems and bone tissue engineering', *Chem. Eur. J.*, 2006, **12**, (23), 5934–5943.
3. L. L. Hench, J. R. Jones and M. B. Fenn: 'New materials and technologies for healthcare', 2011, London, Imperial College Press.
4. L. C. Gerhardt and A. R. Boccaccini: 'Bioactive glass and glass-ceramic scaffolds for bone tissue engineering', *Materials*, 2010, **3**, (7), 3867–3910.
5. J. M. Polak, L. L. Hench and P. Kemp: 'Future strategies for tissue and organ replacement', 2002, Imperial College Press, London.
6. L. L. Hench: 'The story of Bioglass', *J. Mater. Sci. Mater. Med.*, 2006, **17**, (11), 967–978.
7. R. J. Jones: 'Review of bioactive glass: from Hench to hybrids', *Acta Biomater.*, 2013, **9**, (11), 4457–4486.
8. G. Heness and B. Ben-Nissan: 'Innovative bioceramics', *Mater. Forum*, 2004, **27**, 104–114.
9. A. Hoppe, N. S. Güldal and A. R. Boccaccini: 'A review of the biological response to ionic dissolution products from bioactive glasses and glass-ceramic', *Biomaterials*, 2011, **32**, (11), 2757–2774.
10. L. L. Hench: 'Bioceramics: from concept to clinic', *J. Am. Ceram. Soc.*, 1991, **74**, (7), 1487–1510.
11. O. Peitl, E. D. Zanotto and L. L. Hench: 'Highly bioactive P2O5-Na2O-CaO-SiO2 glass-ceramics', *J. Non-Cryst. Solids*, 2001, **292**, 115–126.
12. O. Peitl, E. D. Zanotto, S. C. Serbena and L. L. Hench: 'Compositional and microstructural design of highly bioactive P2O5-Na2O-CaO-SiO2 glass-ceramics', *Acta Biomater.*, 2012, **8**, (1), 321–332.
13. J. R. Jones, L. M. Ehrenfried and L. L. Hench: 'Optimizing bioactive glass scaffolds for bone tissue engineering', *Biomaterials*, 2006, **27**, (7), 964–973.
14. J. E. Gough, J. R. Jones and L. L. Hench: 'Nodule formation and mineralisation of human primary osteoblasts cultured on a porous bioactive glass scaffolds', *Biomaterials*, 2004, **25**, (11), 2039–2046.
15. J. R. Jones, O. Tsigkou, E. E. Coates, M. M. Stevens, J. M. Polak and L. L. Hench: 'Extracellular matrix formation and mineralisation on a phosphate-free porous bioactive glass scaffold using primary human osteoblast (HOB) cells', *Biomaterials*, 2007, **28**, (9), 1653–1663.
16. Q. Z. Chen, I. D. Thompson and A. R. Boccaccini: '45S4 Bioglass-derived glass ceramic scaffolds for bone tissue engineering', *Biomaterials*, 2006, **27**, (11), 2414–2425.
17. Q. Chen, D. Mohn and W. J. Stark: 'Optimization of Bioglass® scaffold fabrication process', *J. Am. Ceram. Soc.*, 2011, **94**, 4184–4190.
18. A. Studart, U. T. Gonzenbach, E. Tervoort and L. J. Gauckler: 'Processing routes to macroporous ceramics: a review', *J. Am. Ceram. Soc.*, 2006, **89**, 1771–1789.
19. K. Rezwan, Q. Z. Chen, J. J. Blaker and A. R. Boccaccini: 'Biodegradable and bioactive porous polymer/inorganic composite scaffolds for bone tissue engineering', *Biomaterials*, 2006, **27**, (18), 3413–3431.
20. J. J. Jones and L. L. Hench: 'Regeneration of trabecular bone using porous ceramics', *Curr. Opin. Solid State Mater. Sci.*, 2003, **7**, 301–307.
21. T. Fukasawa, Z. Y. Deng, M. Ando, T. Ohji and Y. Goto: 'Pore structure of porous ceramics synthesized from water-based slurry by freeze-dry process', *J. Mater. Sci.*, 2001, **36**, (10), 2523–2527.
22. K. F. Leong, C. M. Cheah and C. K. Chua: 'Solid freeform fabrication of three-dimensional scaffolds for engineering replacement tissues and organs', *Biomaterials*, 2003, **24**, (13), 2363–2378.
23. E. A. Aguilar-Reyes, C. A. Leon-Patino, B. Jacinto-Diaz and L. P. Lefebvre: 'Structural characterization and mechanical evaluation of bioactive glass 45S5 foams obtained by a powder technology approach', *J. Am. Ceram. Soc.*, 2012, **95**, (12), 3776–3780.
24. E. A. Aguilar-Reyes, C. A. Leon-Patino, B. Jacinto-Diaz and L. P. Lefebvre: 'Synthesis of 45S5 Bioglass® foams by a powder metallurgy approach', *Mater. Sci. Technol.*, 2010, **17**, 70–77.
25. E. Cunningham, N. Dunne, S. Clarke, S. Y. Choi, G. Walker, R. Wilcox, R. E. Unger, F. Buchnan and C. J. Kirkpatrick: 'Comparative characterization of 3-D hydroxyapatite scaffolds developed via replication of synthetic polymer foams and natural marine sponges', *J. Tissue Sci. Eng.*, 2011, S1:001, doi:10.4172/2157-7552.S1-001.
26. S. Yang, K. F. Leong, Z. Du and C. K. Chua: 'The design of scaffolds for use in tissue engineering—traditional factors', *Tissue Eng.*, 2001, **7**, (6), 679–689.
27. M. Mastrogiacomo, S. Scaglione, R. Martinetti, L. Dolcini, F. Beltrame, R. Cancedda and R. Quarto: 'Role of scaffold internal structure on in vivo bone formation in macroporous calcium phosphate bioceramics', *Biomaterials*, 2006, **27**, 3230–3237.
28. Z. C. Chen, X. L. Zhang, K. Zhou, H. Cai and C. Q. Liu: 'Novel fabrication of hierarchically porous hydroxyapatite scaffolds with refined porosity and suitable strength', *Adv. Appl. Ceram.*, 2015, **114**, (3), 183–187.
29. G. Li, G. Liang, S. Zhao, K. Ma, W. Feng, D. Zhou and X. Liu: 'Synthesis and characterisation of porous luminescent glass ceramic scaffolds containing europium for bone tissue engineering', *Adv. Appl. Ceram.*, 2015, **114**, (3), 164–174.
30. R. Pronzato and R. Manconi: 'Mediterranean commercial sponges: over 5000 years of natural history and cultural heritage', *Mar. Ecol.*, 2008, **29**, 146–166.
31. L. L. Hench and J. Wilson: 'Surface-active biomaterials', *Science*, 1984, **226**, 630–636.
32. L. Lefebvre, J. Chevaliera, R. Gremillarda, R. Zenatib, G. Tholleta, D. Bernache-Assolantc and A. Govinc: 'Structural transformations of bioactive glass 45S5 with thermal treatments', *Acta Biomater.*, 2007, **55**, 3305–3313.
33. D. Clupper D, J. J. Mecholsky, G. P. LaTorre and D. C. Greenspan: 'Sintering temperature effects on the *in vitro* bioactive response of tape cast and sintered bioactive glass-ceramic in TRIS buffer', *J. Biomed. Mater. Res.*, 2001, **57**, 532–540.
34. L. Lefebvre, L. Gremillard, J. Chevaliera, R. Zenatib and D. Bernache-Assolantc: 'Sintering behaviour of 45S5 bioactive glass', *Acta Biomater.*, 2008, **26**, 1665–1674.
35. A. Philippart, A. R. Boccaccini, C. Fleck, D. W. Schubert and J. A. Roether: 'Toughening and functionalization of bioactive ceramic and glass bone scaffolds by biopolymer coatings and infiltration: a review of the last 5 years', *Expert Rev. Med. Devices*, 2015, **12**, 93–111.
36. A. R. Boccaccini, Q. Chen, L. Lefebvre, L. Gremillard and J. Chevalier: 'Sintering, crystallization and biodegradation behavior of Bioglass®-derived glass-ceramic', *Faraday Discuss.*, 2007, **136**, 27–44.